

Spectrum, radial wave functions, and hyperfine splittings of the Rydberg states in heavy-metal alkali atoms

Ali Sanayei and Nils Schopohl*

Institut für Theoretische Physik and CQ Center for Collective Quantum Phenomena and their Applications in LISA⁺, Eberhard-Karls-Universität Tübingen, Auf der Morgenstelle 14, D-72076 Tübingen, Germany and

(Dated: July 14, 2016)

We present numerically accurate calculations of the bound state spectrum of the highly excited valence electron in the heavy-metal alkali atoms solving the radial Schrödinger eigenvalue problem with a modern spectral collocation method that applies also for a large principal quantum number $n \gg 1$. As an effective single-particle potential we favor the reputable potential of Marinescu *et al.*, [Phys. Rev. A **49**, 982 (1994)]. Recent quasiclassical calculations of the quantum defect of the valence electron agree for orbital angular momentum $l = 0, 1, 2, \dots$ overall remarkably well with the results of the numerical calculations, but for the Rydberg states of rubidium and also cesium with $l = 3$ this agreement is less fair. The reason for this anomaly is that in rubidium and cesium the potential acquires for $l = 3$ deep inside the ionic core a second classical region, thus invalidating a standard WKB calculation with two widely spaced turning points. Comparing then our numerical solutions of the radial Schrödinger eigenvalue problem with the uniform analytic WKB approximation of Langer constructed around the remote turning point $r_{n,j,l}^{(+)}$ we observe everywhere a remarkable agreement, apart from a tiny region around the inner turning point $r_{n,j,l}^{(-)}$. For s -states the centrifugal barrier is absent and no inner turning point exists, $r_{n,j,0}^{(-)} = 0$. With the help of an ansatz proposed by Fock we obtain for the s -states a second uniform analytic approximation to the radial wave function complementary to the WKB approximation of Langer, which is exact for $r \rightarrow 0^+$. From the patching condition, that for $l = 0$ the Langer- and Fock solutions should agree in the intermediate region $0 < r \ll r_{n,j,l}^{(+)}$, not only an equation determining the quasiclassical quantum defect δ_0 but also the value of the radial s -wave function at $r = 0$ is analytically found, thus validating the Fermi-Segrè formula for the hyperfine splitting constant $A_{n,j,0}^{(\text{HFS})}$. As an application we consider recent spectroscopic data for the hyperfine splittings of the isotopes ^{85}Rb and ^{87}Rb and find a remarkable agreement with the predicted scaling relation $A_{n,j,0}^{(\text{HFS})} (n - \delta_0)^3 = \text{const.}$

PACS numbers: 31.10.+z, 31.15.-p, 31.30.Gs, 32.80.Ee

I. INTRODUCTION

The alkali atoms have a simple ground state electronic structure, with only one valence electron in an s -state. On a level of accuracy, where the relativistic corrections to the spectrum can be ignored, the bound state spectrum of the excited valence electron can be well described by the spherically symmetric effective single-particle potential of Marinescu *et al.* [1, 2]:

$$V_{\text{eff}}(r; l) = -2 \frac{Z_{\text{eff}}(r; l)}{r} - \alpha_c \frac{1 - \exp\left(-\left(\frac{r}{r_c(l)}\right)^6\right)}{r^4}, \quad (1)$$

where

$$Z_{\text{eff}}(r; l) = 1 + (Z - 1) e^{-ra_1(l)} - r e^{-ra_2(l)} [a_3(l) + ra_4(l)]. \quad (2)$$

This is actually a nonlocal potential, because it depends for each proton number Z of the alkali atom under consideration parametrically on the orbital angular momentum

$l = 0, 1, 2, 3, \dots$ of the valence electron. At small distance r to the atomic nucleus this effective interaction potential mutates into a Coulomb potential, describing the interaction of Z protons with the outermost electron, and an additional (large) constant; that is [2],

$$V_{\text{eff}}(r; l) \rightarrow -\frac{2Z}{r} + 2[(Z - 1)a_1(l) + a_3(l)] \quad \text{for } r \ll 1. \quad (3)$$

Conversely, far outside the ionic core region the potential converts into a superposition of a long-ranged Coulomb term, describing the interaction between a net positive charge $Z - (Z - 1) = 1$ and the valence electron (like in hydrogen atom), and a short-ranged core polarization term; that is [2],

$$V_{\text{eff}}(r; l) \rightarrow -\frac{2}{r} - \frac{\alpha_c}{r^4} \quad \text{for } r \gg 1. \quad (4)$$

In the region around the ionic core, comprising $Z - 1$ strongly bound electrons filling the inner electron shells of the atom, the two parameters α_c and $r_c(l)$ represent the effects of the polarizability of the latter, while the parameters $a_1(l)$, $a_2(l)$, $a_3(l)$, and $a_4(l)$ shape the spatial dependence of the effective charge $Z_{\text{eff}}(r; l)$, as it alters as a function of r from unity to a value Z . For rubidium $Z = 37$, for cesium $Z = 55$, and for francium $Z = 87$.

* nils.schopohl@uni-tuebingen.de

Recently, a phenomenological modification of the potential for $l = 1, 2$ has been suggested in terms of a cutoff $r_{\text{so}}(l)$ in the core region, which successfully predicts for all principal quantum numbers n and total angular momentum $j = l \pm 1/2$ the fine splittings of the Rydberg levels [2, 3]:

$$V_{\text{mod}}(r; j, l) = \begin{cases} V_{\text{eff}}(r; l) & \text{if } 0 \leq r \leq r_{\text{so}}(l), \\ V_{\text{eff}}(r; l) + V_{\text{SO}}(r; j, l) & \text{if } r > r_{\text{so}}(l), \end{cases} \quad (5)$$

where $V_{\text{SO}}(r; j, l)$ denotes the spin-orbit potential. New precise spectroscopic data of ^{87}Rb indeed comply for all principal quantum numbers $n > 7$ very well with the (semi) analytical results obtained from quasiclassical WKB calculations, cf. Tables I and II in Ref. [3].

In what follows, Sec. II, we first check the accuracy of our recent quasiclassical calculations of the spectrum of the highly excited valence electron in ^{87}Rb [3] with the potential (5), employing for the solution of the radial Schrödinger eigenvalue problem a modern numerical collocation method based on the barycentric Chebyshev interpolation [4–6]. The results of these numerical calculations indeed agree very well with our recent quasiclassical calculations of the quantum defects for orbital angular momentum $l = 0, 1, 2$ and also $l \geq 4$, but for $l = 3$ we spot for the heavy-metal alkali atoms rubidium and cesium a discrepancy. In Sec. III we then provide an explanation for this discrepancy bringing out for $l = 3$ a hitherto unnoticed feature of the reputable potential of Marinescu *et al.* (1). In Sec. IV we show how to construct for the radial eigenfunctions of the Rydberg states carrying an arbitrary orbital angular momentum $l \geq 0$ two complementary uniform quasiclassical approximations. The first is the uniform WKB approximation of Langer [7], where we determine the normalization constant by the procedure described by Bender and Orszag [8]. The obtained analytical formula for the radial eigenfunctions of the Rydberg states for $l = 0, 1, 2, \dots$ in fact agrees remarkably well with the numerical calculations almost everywhere with exception of a small region around the origin at $r = 0$. Close to the origin, however, the Langer approximation becomes invalid. We thus patch in the region well below the remote turning point the quasiclassical approximation of Langer with an ansatz for the radial wave function in terms of a Bessel function first proposed by Fock [9], that is asymptotically exact for $r \rightarrow 0^+$, thus enabling us, for example for $l = 0$, to analytically determine at the origin $r = 0$ the value of the radial wave function for the highly excited s -states. In Sec. V, finally, we use these results to present a simple elementary proof for the semi-empirical Fermi-Segrè formula [10] determining the hyperfine splittings of the highly excited s -states of the alkali atoms.

II. SPECTRAL COLLOCATION ON A CHEBYSHEV GRID: A NUMERICALLY ACCURATE METHOD FOR THE SOLUTION OF THE RADIAL SCHRÖDINGER EIGENVALUE PROBLEM

To verify the accuracy of the quasiclassical calculations presented in Ref. [3] a numerically accurate method (see supplementary material [11]) is required, that solves the radial Schrödinger eigenvalue problem for the radial eigenfunctions $R_{n,j,l}(r) = \frac{1}{r} U_{n,j,l}(r)$ with the modified potential (5) reliably and accurately also for large principal quantum numbers $n \gg 1$ [2]:

$$\left[-\frac{d^2}{dr^2} + \frac{l(l+1)}{r^2} + V_{\text{mod}}(r; j, l) - E_{n,j,l} \right] U_{n,j,l}(r) = 0. \quad (6)$$

To achieve this goal we use here a spectral collocation method [4–6] on a grid consisting of $k_{\text{max}} + 1$ Chebyshev grid points obtained by projecting equally spaced points on the unit circle down to the interval $[-1, 1]$. Trivial scaling and shift leads then to the not-equally spaced point set

$$r_k = r_{\text{max}} \frac{1 - \cos\left(\pi \frac{k}{k_{\text{max}}}\right)}{2}, \quad 0 \leq k \leq k_{\text{max}}, \quad (7)$$

which clusters near $r = 0$ and near $r = r_{\text{max}}$. In sharp contrast to a traditional finite difference method that controls the error of numerical discretization by the choice of grid spacing, the accuracy of a *spectral* collocation method (a well-known concept in modern numerical mathematics) is only limited by the smoothness of the function being approximated [4, 11]. Implementing now spectral Chebyshev collocation the sought wave function $U_{n,j,l}(r) = rR_{n,j,l}(r)$ solving the radial Schrödinger eigenvalue problem (6) is represented in terms of a finite vector $U_{n,j,l}(r_k)$ of its values at the Chebyshev grid points r_k , thus defining implicitly a stable and accurate Lagrange polynomial interpolant of degree k_{max} . Of particular value and simplicity is the numerically robust barycentric representation of this interpolant due to Salzer [4]:

$$u_{n,j,l}(r) = \frac{\sum_{k=0}^{k_{\text{max}}} w_k \frac{U_{n,j,l}(r_k)}{r-r_k}}{\sum_{k'=0}^{k_{\text{max}}} \frac{w_{k'}}{r-r_{k'}}}, \quad (8)$$

where

$$w_k = (-1)^k \times \begin{cases} \frac{1}{2} & \text{if } k = 0 \text{ or } k = k_{\text{max}}, \\ 1 & \text{otherwise.} \end{cases} \quad (9)$$

As a matter of fact, $u_{n,j,l}(r)$ is a polynomial of degree k_{max} , coinciding with the function values $U_{n,j,l}(r_k)$ at

the grid points r_k . Well-known accuracy and stability concerns regarding convergence of high order polynomial interpolants do not apply to a Chebyshev grid with its not-equispaced points clustering around the corner points of the grid [4].

Replacing the function $U_{n,j,l}(r)$ by such a polynomial interpolant $u_{n,j,l}(r)$ of degree k_{\max} implies that derivative operations on those functions are replaced by the same operations applied to their interpolant. Thus, the first derivative $\frac{d}{dr}U_{n,j,l}(r)$ is now represented by a matrix $\mathbf{D}^{(1)}$ of size $(k_{\max} + 1) \times (k_{\max} + 1)$ acting on the vector of function values $U_{n,j,l}(r_k)$ at $k_{\max} + 1$ grid points r_k [5], likewise the second-order derivative $\frac{d^2}{dr^2}U_{n,j,l}(r)$ is represented by a matrix $\mathbf{D}^{(2)} = \mathbf{D}^{(1)} \circ \mathbf{D}^{(1)}$. This approach converts the radial Schrödinger eigenvalue problem (6) into a standard matrix eigenvalue problem.

A crucial point here is that in the calculations of the spectrum of the highly excited bound valence electron the grid should be fine enough to resolve the oscillations of the wave functions $U_{n,j,l}(r)$ under consideration also in the coarsest part of the grid in accordance with the sampling theorem [12]. Moreover, the largest grid point r_{\max} should be located in the region well beyond the remote classical turning point $r_{n,j,l}^{(+)} \simeq 2/(-E_{n,j,l})$, say, $r_{\max} \simeq \frac{3}{2}r^{(+)}$. In effect, one then requires Dirichlet boundary conditions for the eigenfunction $U_{n,j,l}(r)$ at both ends of the grid:

$$U_{n,j,l}(0) = 0 = U_{n,j,l}(r_{\max}). \quad (10)$$

These boundary conditions imply that the first and the last columns as well as the first and the last row of the matrix $\mathbf{D}^{(2)}$ can be stripped off [5], thus leading to a $(k_{\max} - 1) \times (k_{\max} - 1)$ matrix eigenvalue problem to be solved for the $k_{\max} - 1$ unknown function values $U_{n,j,l}(r_k)$ at the inner points of the grid.

It should be noted that only eigenvectors with associated eigenvalue $-1 < E_{n,j,l} < 0$ need to be searched [2]. Moreover, because only eigenvectors with components $U_{n,j,l}(r_k)$ becoming exponentially small for r_k well beyond the remote classical turning point $r_{n,j,l}^{(+)}$ are meaningful, all other solutions of the discrete matrix eigenvalue problem being physically meaningless.

For a detailed discussion and demonstration of the accuracy of the spectral collocation method on a Chebyshev grid, we refer to our supplementary material [11], where we present a comparison with the well-known analytical eigenfunctions of the hydrogen atom.

III. THE QUANTUM DEFECT OF THE RYDBERG STATES IN RUBIDIUM AND THE $l = 3$ ANOMALY IN RUBIDIUM AND CESIUM

The bound state spectrum of the valence electron in ^{87}Rb , as calculated by the aforementioned spectral collocation method [11], indeed agrees for almost all orbital angular momenta l , as well with the spectroscopic data

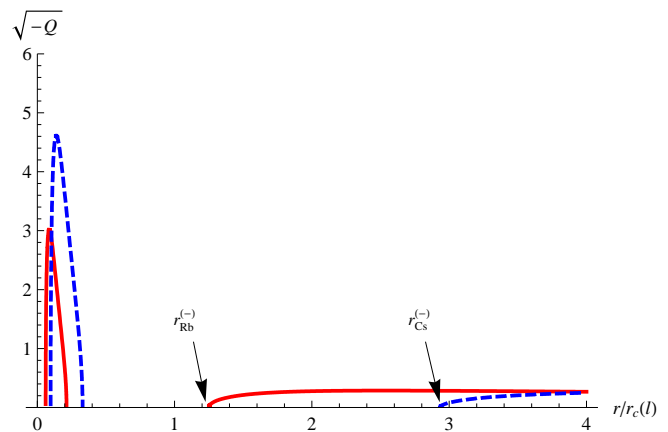


Figure 1. (Color online) The quasiclassical momentum $\sqrt{-Q_{n,j,l}(r)}$ vs. scaled distance $r/r_c(l)$ for orbital angular momentum $l = 3$ and total angular momentum $j = 7/2$ of the excited bound valence electron ($n \gg 1$) for rubidium (red) and cesium (dashed blue) atoms, calculated with the effective potential of Marinescu *et al.* (1). There exists a tiny second classical region located deep inside the atom core close to the origin, where the quasiclassical momentum acquires again real values, well below the positions of the inner turning points $r_{\text{Rb}}^{(-)}$ and $r_{\text{Cs}}^{(-)}$ for rubidium and cesium, respectively, representing the lower boundary of their respective outer classical regions extending up to their remote turning point $r_{n,j,l}^{(+)}$.

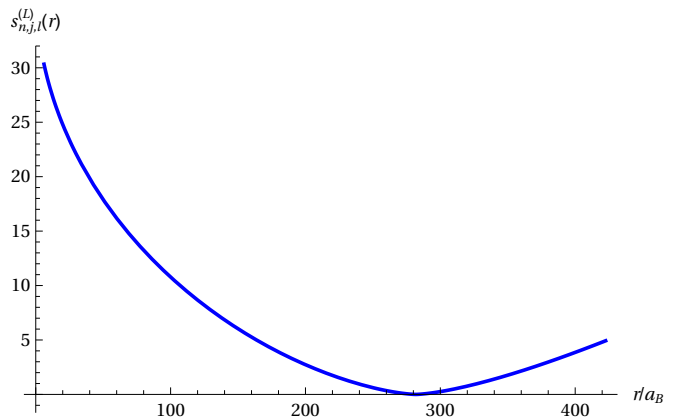


Figure 2. (Color online) The Langer action integral $S_{n,j,l}^{(L)}(r)$, cf. (16), as calculated from a barycentric polynomial interpolant $s_{n,j,l}^{(L)}(r)$ on a Chebyshev grid, for the excited bound valence electron of ^{87}Rb with principal quantum number $n = 15$, orbital angular momentum $l = 0$, and total angular momentum $j = 1/2$.

[13–15] as with the quasiclassical calculations [3], with the exception of the $l = 3$ Rydberg states [16], where a small systematic discrepancy is discernible between the results obtained by the quasiclassical and the full numerical calculations, cf. Table I. We offer here a simple explanation for this anomaly, that applies only to the heavy alkali atoms rubidium and cesium (and most likely also

to francium), and which to the best of our knowledge has not been reported before.

There exists deep inside the atom core of rubidium and cesium, an this applies as a matter of fact only for orbital angular momentum $l = 3$, a tiny second classical region of the potential (1), see Fig. 1, where the classical (radial) momentum

$$p_{n,j,l}(r) = \sqrt{-Q_{n,j,l}(r)}, \quad (11)$$

with

$$Q_{n,j,l}(r) = \frac{l(l+1)}{r^2} + V_{\text{mod}}(r; j, l) - E_{n,j,l}, \quad (12)$$

acquires as a function of distance r to the origin again real-numbered values. This feature invalidates a standard two-turning-point WKB calculation of the spectrum of the $l = 3$ Rydberg states, where the widely spaced classical interval $r_{n,j,3}^{(-)} < r < r_{n,j,3}^{(+)}$ between the remote turning point $r_{n,j,3}^{(+)}$ and the (second largest) inner turning point $r_{n,j,3}^{(-)} \ll r_{n,j,3}^{(+)}$ is taken into account, ignoring the existence of the tiny second classical region inside the core of the atom for $l = 3$, cf. Fig. 1. Because the asymptotics (3) of the potential reveals in the vicinity of the origin $r = 0$ a large constant term, which by far dominates the energy eigenvalues $E_{n,j,l}$ of the bound valence electron, the classical (radial) momentum inside this second classical region is nearly independent on the energy variable $-1 < E_{n,j,l} < 0$ of the bound states under consideration.

As explained in Ref. [3], the quantum defect $\Delta_{j,l} = \delta_l + \eta_{j,l}$ is connected to the energy eigenvalue $E_{n,j,l}$ of the bound valence electron with principal quantum number $n \gg 1$ and total angular momentum $j = l \pm 1/2$ by [2, 17]

$$E_{n,j,l} = -\frac{1}{(n - \Delta_{j,l})^2}, \quad (13)$$

the fine splittings of the spectrum being thus to leading order proportional to the difference $\Delta_{l-\frac{1}{2},l} - \Delta_{l+\frac{1}{2},l} = \eta_{l-\frac{1}{2},l} - \eta_{l+\frac{1}{2},l}$ of the associated quantum defects [3], cf. Table I.

We find for all principal quantum numbers $n > 7$ that choosing the values of the cutoff $r_{\text{so}}(l)$ in (5) according to the rule [2]

$$r_{\text{so}}(l) \simeq \begin{cases} 0.0286294 \times r_c(l) = 0.043 & \text{for } l = 1, \\ 0.0585394 \times r_c(l) = 0.285 & \text{for } l = 2, \\ 0.135464 \times r_c(l) = 0.650 & \text{for } l = 3, \end{cases} \quad (14)$$

the numerical calculations of the fine splitting agree surprisingly well with the spectroscopic data of [13–16],

cf. Table I. Choosing larger or smaller values for $r_{\text{so}}(l)$ than stated in (14), the calculated fine splittings cease to give better agreement with experiment. Only for orbital angular momentum $l = 3$ we also find that changing the parameter $a_3(l)$ in the effective potential (1) from its tabulated value in Ref. [1] according to the rule $a_3(l = 3) \rightarrow 0.983431 \times a_3(l = 3)$ slightly improves the coincidence between the numerical calculations and spectroscopic data [16, 18]. Note that for the quasiclassical calculation of quantum defect associated with $l = 0$ and $l = 2$, we use the scaling prescription for $a_3(l = 0)$ and $a_3(l = 2)$ according to Ref. [3].

Recently, a calculation of the fine splittings for $l = 3$ in rubidium atoms has been carried out, taking a different potential and using a relativistic many-body perturbation theory that employs relativistic finite basis sets constructed from solutions to the single-electron Dirac equation with a potential [19]. The results of these calculations for the fine splittings of $l = 3$ states in Rb atoms are closer to the experiments [16, 20, 22]. However, we should like to point out a serious consistency problem attempting to solve a relativistic many-particle problem employing a single-electron Dirac equation with a potential $V(r)$ that treats the relative coordinate r as a four-vector, cf. Eq. (1) in Ref. [19]. For a thorough analysis of the relativistic H-atom, we refer to Ref. [21]. A correct approach aiming at taking into account the leading order of relativistic effects in a many-electron problem should, in our opinion, be based on the Breit-Pauli Hamiltonian [23, 24], including not only the usual spin-orbit term, but also the spin-spin interaction term and the spin-other-orbit interaction [3, 24]. Both terms, the spin-spin interaction and the spin-other-orbit interaction, influence the fine splitting as genuine relativistic multi-electron terms which are certainly beyond the terms provided by any single-electron Dirac equation, see Refs. [23, 24] for expanded details.

IV. TWO COMPLEMENTARY UNIFORM QUASICLASSICAL APPROXIMATIONS FOR THE RADIAL EIGENFUNCTIONS

Once an energy eigenvalue $-1 < E_{n,j,l} < 0$ is determined from the quasiclassical quantization condition, the corresponding uniform WKB approximation of Langer to the solution of the radial Schrödinger equation (6), being constructed around the remote turning point $r_{n,j,l}^{(+)}$ is [7, 8]:

Table I. The values of quantum defect $\Delta_{j,l}$ associated with the Rydberg level $n = 15$ for $l = 0, 1, 2, 3, 4$ and $j = l \pm 1/2$. Experimental values for $l = 3, 4$ are related to ^{85}Rb and all theoretical values correspond to ^{87}Rb . An estimation of uncertainties for the values of quantum defect calculated by both quasiclassical theory and numerical collocation spectral method based on the barycentric Chebyshev interpolation was obtained by varying the most effective parameter of the reputable potential (1) to the values of quantum defect [i.e., $a_3(l)$] by around 1%.

Quantum defect $\Delta_{j,l}$	Expt. [13]	Expt. [14]	Expt. [16]	Expt. [15]	Quasiclassical theory [3]	Numerical calculation (this work)
$\Delta_{1/2,0}$	3.132 45(10)	3.132 45(2)	NA	NA	3.131(3)	3.132(3)
$\Delta_{1/2,1}$	2.656 79(10)	NA	NA	NA	2.640(4)	2.659(3)
$\Delta_{3/2,1}$	2.643 58(10)	NA	NA	NA	2.653(4)	2.645(3)
$ \Delta_{1/2,1} - \Delta_{3/2,1} $	0.013 21(14)	NA	NA	NA	0.013(8)	0.013(6)
$\Delta_{3/2,2}$	1.344 86(4)	1.344 85(2)	NA	NA	1.345(9)	1.345(9)
$\Delta_{5/2,2}$	1.343 27(3)	1.343 28(2)	NA	NA	1.347(9)	1.344(9)
$ \Delta_{3/2,2} - \Delta_{5/2,2} $	0.001 59(5)	0.001 57(3)	NA	NA	0.001(18)	0.001(18)
$\Delta_{5/2,3}$	NA	NA	0.016 1406(9)	NA	0.013 400(4)	0.0164(4)
$\Delta_{7/2,3}$	NA	NA	0.016 1606(7)	NA	0.013 404(4)	0.0164(4)
$ \Delta_{5/2,3} - \Delta_{7/2,3} $	NA	NA	0.000 0200(7)	NA	0.000 004(8)	0.000 03(8)
$\Delta_{7/2,4}$	NA	NA	NA	0.004 05(6)	0.005 1500(4)	0.003 8385(4)
$\Delta_{9/2,4}$	NA	NA	NA	0.004 05(6)	0.005 1500(4)	0.003 8385(4)

$$U_{n,j,l}^{(L)}(r) = C_{n,j,l}^{(L)} \left[\frac{3}{2} S_{n,j,l}^{(L)}(r) \right]^{\frac{1}{6}} \left[\text{sgn}(r - r_{n,j,l}^{(+)}) Q_{n,j,l}^{(L)}(r) \right]^{-\frac{1}{4}} \text{Ai} \left(\text{sgn}(r - r_{n,j,l}^{(+)}) \left[\frac{3}{2} S_{n,j,l}^{(L)}(r) \right]^{\frac{2}{3}} \right). \quad (15)$$

The function $\text{Ai}(x)$ denotes the well-known Airy function [8] and $\text{sgn}(x) = |x|/x$. The function $S_{n,j,l}^{(L)}(r)$ is the Langer action integral,

$$S_{n,j,l}^{(L)}(r) = \begin{cases} \int_r^{r_{n,j,l}^{(+)}} dr' \sqrt{-Q_{n,j,l}^{(L)}(r')} & \text{if } r \leq r_{n,j,l}^{(+)} \\ \int_{r_{n,j,l}^{(+)}}^r dr' \sqrt{Q_{n,j,l}^{(L)}(r')} & \text{if } r \geq r_{n,j,l}^{(+)} \end{cases} \quad (16)$$

where the function $\sqrt{-Q_{n,j,l}^{(L)}(r)}$ is the quasiclassical momentum (11), but slightly modified with the centrifugal barrier term being altered taking into account the Langer correction $l(l+1) \rightarrow (l + \frac{1}{2})^2$ [25]:

$$Q_{n,j,l}^{(L)}(r) = \frac{(l + \frac{1}{2})^2}{r^2} + V_{\text{mod}}(r; j, l) - E_{n,j,l}. \quad (17)$$

For $l = 0$ the centrifugal barrier term and the spin-orbit coupling potential $V_{\text{SO}}(r; j, l)$ are both absent, and the lower turning point $r_{n,j,0}^{(-)}$ transforms into a singularity of the radial Schrödinger equation (6), thus preventing a standard two-turning-point WKB calculation of the spectrum. For a rigorous derivation of the normalization constant $C_{n,j,l}^{(L)}$ we refer to Ref. [8]:

$$C_{n,j,l}^{(L)} = (-1)^{n-l-1} \sqrt{\frac{2\pi}{\int_{r_{n,j,l}^{(-)}}^{r_{n,j,l}^{(+)}} \frac{dr}{\sqrt{-Q_{n,j,l}^{(L)}(r)}}}}. \quad (18)$$

In our WKB calculations we determine the positions $r = r_{n,j,l}^{(\pm)}$ of the turning points numerically by solving the implicit equation $Q_{n,j,l}^{(L)}(r) = 0$. For large n there holds approximately

$$r_{n,j,l}^{(+)} \simeq \begin{cases} \frac{2}{-E_{n,j,l}} & \text{if } l = 0, \\ \frac{1}{-E_{n,j,l}} \left[1 + \sqrt{1 + (l + \frac{1}{2})^2 E_{n,j,l}} \right] & \text{if } l \geq 1, \end{cases} \quad (19)$$

and

$$r_{n,j,l}^{(-)} \simeq \begin{cases} 0 & \text{if } l = 0, \\ 0.02 \times r_c(l) & \text{if } l = 1, 2, \\ \frac{(l + \frac{1}{2})^2}{1 + \sqrt{1 + (l + \frac{1}{2})^2 E_{n,j,l}}} & \text{if } l \geq 3. \end{cases} \quad (20)$$

In Fig. 2 the action integral $S_{n,j,l}^{(L)}(r)$ is displayed choosing, for example, $n = 15$, $l = 0$, and $j = 1/2$. Replacing the action integral (16) as a function of the radial variable r in (15) by an accurate barycentric interpolation polynomial on a suitable Chebyshev grid (7), a substantial saving of computer time without any loss of accuracy is attained. We found it advantageous to use in the calculations of the action integral two complementary Chebyshev grids, one with a number k_{max} of grid points r_k in the interval $0 \leq r_k \leq r_{n,j,l}^{(+)}$, the other with

a smaller number k'_{\max} of grid points $r_{k'}$ in the interval $r_{n,j,l}^{(+)} \leq r_{k'} \leq r_{\max}$.

In Fig. 3(a), the (normalized) Chebyshev polynomial interpolant $u_{n,j,l}(r)$ to the radial eigenfunction $U_{n,j,l}(r)$ of the valence electron of ^{87}Rb , as calculated from (8) with the method of spectral collocation on a Chebyshev grid, is plotted for the excited valence electron in ^{87}Rb for principal quantum number $n = 15$, $l = 0$, and $j = 1/2$ [26]. With exception of a small region around the origin a remarkable agreement is evident between the uniform WKB approximant $U_{n,j,l}^{(L)}(r)$ of Langer and the Chebyshev polynomial approximant $u_{n,j,l}(r)$ to the eigenfunction $U_{n,j,l}(r)$.

Excluding a small region near to the lower boundary $r_{n,j,l}^{(-)}$ of the classically accessible region $r_{n,j,l}^{(-)} \leq r \leq r_{n,j,l}^{(+)}$, the uniform WKB solution $U_{n,j,l}^{(L)}(r)$ of Langer approximates for $r > r_{n,j,l}^{(-)}$ the exact eigenfunction $U_{n,j,l}(r)$ of the valence electron in the alkali atoms for arbitrary orbital angular momentum l very well, with the exception of the $l = 3$ states in rubidium and cesium, because of the second classically region inside the core, cf. Fig. 1. The key idea of the uniform WKB approximation of Langer is to replace the spatial variation of the potential around the turning points $r_{n,j,l}^{(\pm)}$ of the classically accessible region by a linear function of r , thus reducing in that region the radial differential equation (6) to an analytically solvable one in terms of the Airy functions. But $r_{n,j,l}^{(-)}$ is zero for $l = 0$, and according to (20) it is very small for $l = 1, 2$. Hence, for orbital angular momentum $l < 4$ the spatial variation of the potential (1), which is near to the origin a Coulomb potential, cf. (3), in fact cannot be approximated well by a linear function of r .

Fortunately, with the help of an ansatz proposed by Fock [9], a second uniform quasiclassical solution to (6) can be constructed, that approximates now close to the origin the exact eigenfunction $U_{n,j,l}(r)$ very well, thus being complementary to the uniform WKB solution (15):

$$U_{n,j,l}^{(F)}(r) = \frac{C_{n,j,l}^{(F)}}{\sqrt{\frac{d}{dr} \ln [s_{n,j,l}(r)]}} J_{2l+1}(s_{n,j,l}(r)). \quad (21)$$

Here $J_k(z)$ denotes a Bessel function of the order k , and the unknown function $s_{n,j,l}(r)$ is chosen such that the differential equation obeyed by the ansatz $U_{n,j,l}^{(F)}(r)$ in the interval $0 \leq r \ll r_{n,j,l}^{(+)}$ coincides with the radial Schrödinger equation (6) for $r \rightarrow 0^+$, see Sec. V.

Figure 3(b) presents an expanded view of the region around the origin, revealing that the uniform WKB approximation of Langer ceases to agree well with the eigenfunction $u_{n,j,l}(r)$ for $r \rightarrow 0^+$. Instead, now a remarkable agreement between $u_{n,j,l}(r)$ with the uniform quasiclassical solution $U_{n,j,l}^{(F)}(r)$, as obtained with the ansatz of Fock, is evident.

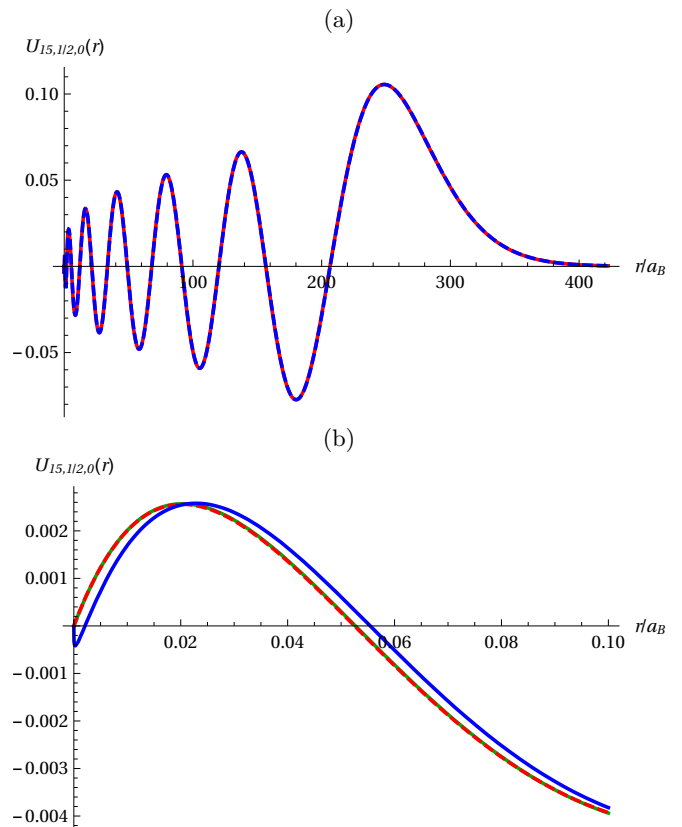


Figure 3. (Color online) (a) The Chebyshev polynomial interpolant $u_{n,j,l}(r)$ to the eigenfunction $U_{n,j,l}(r)$ vs. radial distance r of the excited valence electron in ^{87}Rb for principal quantum number $n = 15$, $l = 0$, and $j = 1/2$ as calculated with the method of spectral collocation on a Chebyshev grid (red line), choosing $r_{\max} = 663.261$ and $k_{\max} = 700$. Also shown is the uniform WKB approximant $U_{n,j,l}^{(L)}(r)$ of Langer (dashed blue), the error $|u_{n,j,l}(r) - U_{n,j,l}^{(L)}(r)|$ being smaller than 10^{-3} for $r > a_B$, cf. Ref. [11]; (b) Expanded view around $r = 0$ of $u_{n,j,l}(r)$ (dashed red), of $U_{n,j,l}^{(L)}(r)$ (blue) and of the uniform quasiclassical approximant $U_{n,j,l}^{(F)}(r)$ of Fock (green), the error $|u_{n,j,l}(r) - U_{n,j,l}^{(F)}(r)|$ being smaller than 10^{-7} for $r < 3 \times a_B$, for further details see Ref. [11].

V. QUASICLASSICAL WAVE FUNCTIONS AND HYPERFINE SPLITTINGS OF THE RYDBERG S -STATES

We want to find out how the size of the hyperfine splittings of the Rydberg s -states depends on the principal quantum number n and on the quantum defect δ_0 . Due to the absence of the centrifugal barrier and zero spin-orbit coupling for $l = 0$ and $j = 1/2$, the associated exact radial wave function $U_{n,j,0}(r) = rR_{n,j,0}(r)$ solving the Schrödinger eigenvalue problem (6) becomes near to the origin a linear function of r . Thus, it is required that the quasiclassical approximation $U_{n,j,0}^{(F)}(r)$ to $U_{n,j,0}(r)$ obeys

to the boundary-value condition

$$\lim_{r \rightarrow 0^+} \frac{U_{n,j,0}^{(F)}(r)}{r} = \lim_{r \rightarrow 0^+} \frac{dU_{n,j,0}^{(F)}(r)}{dr} = R_{n,j,0}^{(F)}(0) = \text{const.} \quad (22)$$

The task is to determine that constant $R_{n,j,0}^{(F)}(0)$ within the quasiclassical theory. A straightforward calculation shows that the function $U_{n,j,0}^{(F)}(r)$ defined in (21) solves the differential equation

$$\left[-\frac{d^2}{dr^2} + Q_{n,j,0}^{(F)}(r) \right] U_{n,j,0}^{(F)}(r) = 0, \quad (23)$$

provided that

$$Q_{n,j,0}^{(F)}(r) = - \left[s_{n,j,0}^{(1)}(r) \right]^2 + \frac{3}{4} \left[\frac{s_{n,j,0}^{(1)}(r)}{s_{n,j,0}^{(1)}(r)} \right]^2 + \frac{3}{4} \left[\frac{s_{n,j,0}^{(2)}(r)}{s_{n,j,0}^{(1)}(r)} \right]^2 - \frac{1}{2} \frac{s_{n,j,0}^{(3)}(r)}{s_{n,j,0}^{(1)}(r)}. \quad (24)$$

Here $f^{(k)}(r) \equiv \frac{d^k}{dr^k} f(r)$ denotes the derivative of order $k = 1, 2, 3, \dots$ of a function $f(r)$. The choice

$$s_{n,j,0}(r) = S_{n,j,0}^{(F)}(r) \equiv \int_0^r dr' \sqrt{-Q_{n,j,0}(r')}, \quad (25)$$

with

$$Q_{n,j,0}(r) = V_{\text{eff}}(r; l=0) - E_{n,j,0}, \quad (26)$$

leads now to the identification

$$Q_{n,j,0}^{(F)}(r) = Q_{n,j,0}(r) - \frac{3}{4} \frac{Q_{n,j,0}(r)}{\left[S_{n,j,0}^{(F)}(r) \right]^2} + \frac{5}{16} \left[\frac{Q_{n,j,0}^{(1)}(r)}{Q_{n,j,0}(r)} \right]^2 - \frac{1}{4} \frac{Q_{n,j,0}^{(2)}(r)}{Q_{n,j,0}(r)}. \quad (27)$$

For $r \rightarrow 0^+$ the residue vanishes, that is $\frac{Q_{n,j,0}^{(F)}(r) - Q_{n,j,0}(r)}{Q_{n,j,0}(r)} \rightarrow 0$, implying that the Fock ansatz (21) represents for $l=0$ inside the classically accessible interval $0 \leq r < r_{n,j,0}^{(+)}$ a second uniform approximation to the solution of the radial Schrödinger equation (6). The uniform quasiclassical solution of Fock, which we present for $l=0$ now in the guise

$$U_{n,j,0}^{(F)}(r) = C_{n,j,0}^{(F)} \frac{\sqrt{S_{n,j,0}^{(F)}(r)}}{[-Q_{n,j,0}(r)]^{\frac{1}{4}}} J_1 \left(S_{n,j,0}^{(F)}(r) \right), \quad (28)$$

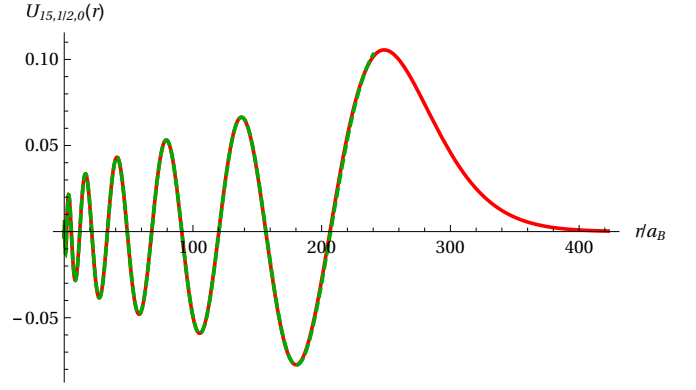


Figure 4. (Color online) Comparison of the Chebyshev polynomial approximant $u_{n,j,l}(r)$ to the normalized eigenfunction $U_{n,j,l}(r)$ as calculated with the method of spectral collocation on a Chebyshev grid (red line), choosing $r_{\text{max}} = 663.261$ and $k_{\text{max}} = 700$, with the uniform Fock ansatz (dashed green) associated with the bound valence electron in ^{87}Rb for the Rydberg level with principal quantum number $n = 15$, $l = 0$, and $j = 1/2$.

indeed approximates inside the classically accessible region $0 \leq r < r_{n,j,0}^{(+)}$ the exact eigenfunctions $U_{n,j,0}(r)$ of the Rydberg s -states of the valence electron in the alkali atoms very well, almost up to the remote turning point $r_{n,j,0}^{(+)}$, see Fig. 4.

Deep inside the classically accessible region $0 \ll r \ll r_{n,j,0}^{(+)}$ both action integrals, $S_{n,j,0}^{(F)}(r)$ and $S_{n,j,0}^{(L)}(r)$, see (25) and (16), assume for $n \gg 1$ large values, so that the well-known asymptotics of the Bessel function $J_1(z)$ and of the Airy function $\text{Ai}(-z)$, valid for large arguments $z \gg 1$, can be used [27]:

$$\text{Ai}(-z) \rightarrow \frac{1}{\sqrt{\pi}} \frac{\cos\left(\frac{2}{3}z^{\frac{3}{2}} - \frac{\pi}{4}\right)}{z^{\frac{1}{4}}}, \quad (29)$$

and

$$J_1(z) \rightarrow \sqrt{\frac{2}{\pi z}} \cos\left(z - \frac{3}{4}\pi\right). \quad (30)$$

Accordingly, the uniform approximations of Langer (15) and of Fock (28) respectively simplify in that region to

$$U_{n,j,0}^{(L)}(r) \rightarrow \frac{C_{n,j,0}^{(L)}}{\sqrt{\pi}} \frac{\cos\left(S_{n,j,0}^{(L)}(r) - \frac{\pi}{4}\right)}{[-Q_{n,j,0}(r)]^{\frac{1}{4}}}, \quad (31)$$

and

$$U_{n,j,0}^{(F)}(r) \rightarrow C_{n,j,0}^{(F)} \sqrt{\frac{2}{\pi}} \frac{\cos\left(S_{n,j,0}^{(F)}(r) - \frac{3}{4}\pi\right)}{[-Q_{n,j,0}(r)]^{\frac{1}{4}}}. \quad (32)$$

The patching requirement that both functions $U_{n,j,0}^{(L)}(r)$ and $U_{n,j,0}^{(F)}(r)$ should coincide for $0 \ll r \ll r_{n,j,0}^{(+)}$ can only be fulfilled provided that

$$S_{n,j,0}^{(F)}(r) + S_{n,j,0}^{(L)}(r) = \int_0^{r_{n,j,0}^{(+)}} dr' \sqrt{-Q_{n,j,0}(r')} = n\pi, \quad (33)$$

and

$$C_{n,j,0}^{(F)} = \frac{(-1)^{n-1}}{\sqrt{2}} C_{n,j,0}^{(L)}. \quad (34)$$

Equation (33) is the quasiclassical quantization condition for zero orbital angular momentum $l = 0$ [3, 28], determining here the energy levels of the Rydberg s -states [2]

$$E_{n,j,0} = -\frac{1}{(n - \delta_0)^2}, \quad (35)$$

with $\delta_0 \equiv \Delta_{1/2,0}$ the quantum defect of the valence electron for $l = 0$. It turns out that (28) is a very good approximation to the eigenfunction $U_{n,j,0}(r)$ everywhere in the classically accessible region below the remote turning point, cf. Fig. 4.

The normalization constant (18) for $l = 0$ can also be expressed analytically in terms of the quantum defect δ_0 . To see this, let us write for the moment being the remote turning point $r_{n,j,0}^{(+)}$ as a function of the energy variable E , i.e., the function $r^{(+)}(E)$ is determined from the requirement

$$E - V_{\text{eff}}(r^{(+)}(E); l = 0) = 0. \quad (36)$$

We now rewrite (18) in the guise

$$\frac{1}{|C_{n,j,0}^{(L)}|^2} = \lim_{E \rightarrow E_{n,j,0}} \frac{d}{dE} \nu(E), \quad (37)$$

with $\nu(E)$ denoting the action integral [3]

$$\nu(E) = \frac{1}{\pi} \int_0^{r^{(+)}(E)} dr' \sqrt{E - V_{\text{eff}}(r'; l = 0)}. \quad (38)$$

With the help of the relation $\frac{d}{dE} \nu(E) = \frac{1}{dE/d\nu}$ and taking into account the identity $\lim_{E \rightarrow E_{n,j,0}} \nu(E) = n$, cf. (33), there follows from (34) at once for $l = 0$ and $j = 1/2$:

$$\left| C_{n,j,0}^{(F)} \right|^2 = \frac{1}{2} \left| C_{n,j,0}^{(L)} \right|^2 = \frac{1}{2} \frac{d}{dn} E_{n,j,0} = \frac{1 - \frac{d}{dn} \delta_0}{(n - \delta_0)^3}. \quad (39)$$

For the $l = 0$, $j = 1/2$ states of the valence electron in the alkali atoms the fine structure splitting due to spin-orbit coupling (assuming exact spherical symmetry of the effective potential) is zero. Neglecting the electric quadrupole moment of the nucleus a detectable shift in the spectrum can now be attributed to the hyperfine interaction of the magnetic moment of the valence electron with the nuclear magnetic moment [29]. Within the

range of validity of the Fermi-contact-interaction model, the size of the spectral splitting is then determined by the magnetic dipole interaction (hyperfine splitting) constant [29]

$$A_{n,j,0}^{(\text{HFS})} = \frac{2}{3} \mu_0 g_s \tilde{g}_I \mu_B^2 \lim_{|\mathbf{r}| \rightarrow 0^+} |\psi_{n,j,0}(\mathbf{r})|^2. \quad (40)$$

Here μ_0 is the vacuum permeability, $\mu_B = \frac{|e|\hbar}{2m_e}$ denotes the Bohr magneton, and the g -factors of electron and nucleus are $g_s = 2.0023193043622$ and $\tilde{g}_I = \frac{m_e}{m_p} g_I$, respectively. For ^{87}Rb it is found that $\tilde{g}_I = -0.0009951414$, and for ^{85}Rb , $\tilde{g}_I = -0.00029364000$ [30]. It should be noted that in our system of units, see [2], the particle density distribution $|\psi_{n,j,0}(\mathbf{r})|^2$ is being measured as the number of particles per unit volume $(a_B)^3$.

The value of the wave function of the Rydberg s -states $\psi_{n,j,0}(\mathbf{r}) = R_{n,j,0}(r) Y_{0,0}(\vartheta, \varphi)$ at the origin $r = 0$ can be calculated analytically using the asymptotics of the action integral (25) for small r :

$$S_{n,j,0}^{(F)}(r) \rightarrow \sqrt{8Zr} + \mathcal{O}\left(r^{\frac{3}{2}}\right). \quad (41)$$

Insertion of (41) into (28) leads then together with the analytical result (39) for the normalization constant to the exact result

$$\begin{aligned} \lim_{|\mathbf{r}| \rightarrow 0^+} |\psi_{n,j,0}(\mathbf{r})|^2 &= \lim_{r \rightarrow 0^+} \left| \frac{U_{n,j,0}^{(F)}(r)}{r} \frac{1}{\sqrt{4\pi}} \right|^2 \\ &= \frac{Z}{\pi} \frac{1 - \frac{d}{dn} \delta_0}{(n - \delta_0)^3}. \end{aligned} \quad (42)$$

This formula connects the value of the s -state wave function at the origin to the derivative $\frac{d}{dn} E_{n,j,0}$ of the bound state spectrum in a radial Schrödinger eigenvalue problem. In the literature it is often referred to as the semi-empirical Fermi-Segrè formula [9, 10, 31]. For a rigorous derivation for differential equations of the type (6), based on an identity for the Wronski determinant, see Ref. [32].

Equation (40) engenders that the magnetic dipole interaction (hyperfine splitting) constant $A_{n,j,0}^{(\text{HFS})}$ for the highly excited valence electron of the alkali atoms ($d\delta_0/dn \approx 0$) indeed should obey to the scaling relation

$$A_{n,j,0}^{(\text{HFS})} (n - \delta_0)^3 = \text{const.} \quad (43)$$

In experiment the hyperfine level shift depends on nuclear spin I , total angular momentum of the valence electron j , and on total angular momentum F assuming values in the interval $|I - j| \leq F \leq I + j$. If only the magnetic dipole interaction was considered, then for $l = 0$, $j = 1/2$ a level $E_{n,j,0}$ would split as a result of the magnetic hyperfine interaction for the special case of nuclear spin

Table II. Values of the scaled magnetic dipole interaction (hyperfine splitting) constant $\frac{A_{n,j,0}^{(\text{HFS})}}{h} (n - \delta_0)^3$, in gigahertz, associated with the highly excited s -states of the bound valence electron in ^{85}Rb and ^{87}Rb . Experiments [13] and [14] were carried out for principal quantum numbers $n \in \{28, 29, 30, 31, 32, 33\}$, and Experiment [33] for $n \in \{20, 21, 22, 23, 24\}$. Note that an estimation of the uncertainty for the numerical calculation of quantum defect δ_0 (cf. Table I) was obtained by varying the most effective parameter of the reputable potential (1) to the values of quantum defect [i.e., $a_3(0)$] by around 1%.

Isotope	Expt. [13]	Expt. [14]	Expt. [33]	Theory (this work)
^{85}Rb	4.87(14)	NA	NA	5.082(3)
^{87}Rb	NA	16.75(9)	18.55(2)	17.223(3)

$I \geq 1/2$ into a doublet structure with quantum numbers $F = I \pm 1/2$ [29]:

$$\Delta E_{n,j,0}^{(\text{HFS})} = A_{n,j,0}^{(\text{HFS})} \frac{F(F+1) - I(I+1) - j(j+1)}{2}. \quad (44)$$

Table II compares the theoretical values of the magnetic dipole interaction (hyperfine splitting) constant $A_{n,j,0}^{(\text{HFS})}$ obtained from (43) for ^{85}Rb and ^{87}Rb atoms with spectroscopic data [13, 14, 33]. Overall, a very good agreement between theory and experiment can be observed.

VI. CONCLUSIONS

Using a numerically accurate and easy to implement modern numerical method, namely, spectral collocation on a Chebyshev grid [4–6] based on the barycentric interpolation formula of Salzer (8), we solved the radial Schrödinger eigenvalue problem and determined the excitation spectrum of the bound valence electron in the alkali atoms, thus confirming the high accuracy of recent quasiclassical calculations of the quantum defect for the Rydberg states carrying orbital angular momentum $l = 0, 1, 2$ or $l > 3$, with exception of the $l = 3$ Rydberg states of rubidium and cesium atoms. As a reason for this anomaly we identified as a feature of the potential of Marinescu *et al.* [1], existing only for orbital angular momentum $l = 3$, a tiny second classical region located deep inside the atom core around the nucleus of alkali atoms with proton number $Z \geq 37$, cf. Fig. (1), thus invalidating for the heavy alkali atoms, rubidium and cesium (and possibly also francium), a standard WKB calculation with only two widely spaced turning points. Also, we found that the uniform WKB approximation of Langer for the radial wave function of the valence electron for $l \neq 3$ indeed represents almost everywhere a remarkably accurate approximation to the exact solution of the radial Schrödinger eigenvalue problem (6), omitting a tiny

interval near to the lower turning point of the classically accessible region. In the region around the origin, where the uniform WKB approximation of Langer for the s -states ceases to be valid, we then showed using an ansatz of Fock [9], that a complementary uniform quasiclassical solution in terms of a Bessel function can be constructed, that coincides with the exact solution of the radial wavefunction for $r \rightarrow 0^+$. The uniform quasiclassical approximation of Fock for the Rydberg the s -states was found to approximate the exact radial eigenfunction almost everywhere in the classically accessible region remarkably well, with exception of a small interval around the remote turning point. A substantial reduction of computer time was achieved in the evaluations of the quasiclassical wave functions (15) and (28), when we replaced the action integral $S_{n,j,l}^{(\text{L})}(r)$ by a corresponding (high-order) barycentric interpolation polynomials $s_{n,j,l}^{(\text{L})}(r)$ in the interval $0 \leq r \leq r_{\text{max}}$. Upon patching the wave function of Langer and Fock inside the classically accessible region and making use of an exact result for the normalization integral of the Langer wave function, due to Bender and Orszag [8], we finally derived an analytical result determining the quantum defect for $l = 0$ and also the value of the radial s -wave eigenfunctions at the origin, thus providing a very simple and short proof of the Fermi-Segrè formula. Also, within the range of validity of the Fermi-contact model an analytic scaling relation for the constant $A_{n,j,0}^{(\text{HFS})}$ describing the size of the hyperfine shifts and splittings of the Rydberg s -states of the valence electron in alkali atoms was found, cf. (43), that apparently is for all principal quantum numbers $n \gg 1$ in good agreement with precise spectroscopic data of ^{85}Rb and ^{87}Rb .

ACKNOWLEDGMENTS

We thank József Fortágh, Florian Karlewski, Markus Mack, and Jens Grimmel for useful discussions.

[1] M. Marinescu, H. R. Sadeghpour, and A. Dalgarno, Phys. Rev. A **49**, 982 (1994).

[2] We use scaled variables so that length is measured in units of the Bohr radius $a_B = 4\pi\epsilon_0\hbar^2/m_e|e|^2 \simeq 5.2918 \times 10^{-11}\text{m}$, and energy is measured in units of Rydberg,

- $Ry = m_e |e|^4 / 8\epsilon_0^2 h^2 \simeq 13.607\text{eV}$.
- [3] A. Sanayei, N. Schopohl, J. Grimm, M. Mack, F. Karlewski, and J. Fortágh, *Phys. Rev. A* **91**, 032509 (2015).
- [4] L. N. Trefethen, *Approximation Theory and Approximation Practice* (SIAM, Philadelphia, 2013).
- [5] L. N. Trefethen, *Spectral Methods in MATLAB* (SIAM, Philadelphia, 2000).
- [6] J. P. Boyd, *Chebyshev and Fourier Spectral Methods* (Dover, New York, 2001).
- [7] R. E. Langer, *Bull. Am. Math. Soc.* **40**, 545 (1934).
- [8] C. M. Bender and S. A. Orszag, *Advanced Mathematical Methods for Scientists and Engineers* (McGraw-Hill, Singapore, 1978).
- [9] V. A. Fock, *Selected Works* (Chapman & Hall/CRC, New York, 2004), pp. 325-329.
- [10] E. Fermi and E. Segrè, *Z. Physik* **82**, 729 (1933).
- [11] A. Sanayei and N. Schopohl, see supplementary material.
- [12] W. H. Press, S. A. Teukolsky, W. T. Vetterling, and B. P. Flannery, *Numerical Recipes in C: The Art of Scientific Computing*, 2nd ed. (Cambridge University Press, Cambridge, 1992).
- [13] W. Li, I. Mourachko, M. W. Noel, and T. F. Gallagher, *Phys. Rev. A* **67**, 052502 (2003).
- [14] M. Mack, F. Karlewski, H. Hattermann, S. Höck, F. Jessen, D. Cano, and J. Fortágh, *Phys. Rev. A* **83**, 052515 (2011).
- [15] K. Afrousheh, P. Bohlouli-Zanjani, J. A. Pterus, and J. D. D. Martin, *Phys. Rev. A* **74**, 062712 (2006).
- [16] J. Han, Y. Jamil, D. V. L. Norum, P. J. Tanner, and T. F. Gallagher, *Phys. Rev. A* **74**, 054502 (2006).
- [17] T. F. Gallagher, *Rydberg Atoms* (Cambridge University Press, Cambridge, 1994).
- [18] L. A. M. Johnson, H. O. Majeed, B. Sanguinetti, Th. Becker, and B. T. H. Varcoe, *N. J. Phys.* **12**, 063028 (2010).
- [19] S. A. Blundell, *Phys. Rev. A* **90**, 042514 (2014).
- [20] J. R. Brandenberger, C. A. Regal, R. O. Jung, and M. C. Yakes, *Phys. Rev. A* **65**, 042510 (2002).
- [21] A. O. Barut and A. Baiquni, *Phys. Rev.* **184**, 1342 (1969).
- [22] J. R. Brandenberger and G. S. Malyshev, *Phys. Rev. A* **81**, 032515 (2010).
- [23] H. A. Bethe and E. E. Salpeter, *Quantum Mechanics of One- and Two-Electron Atoms* (Springer, Berlin, 1957).
- [24] C. Froese-Fischer, T. Brage, and P. Jönsson, *Computational Atomic Structure: An MCHF Approach* (IOP Physics, Bristol, 1997).
- [25] R. E. Langer, *Phys. Rev.* **51**, 669 (1937).
- [26] For a plot of the eigenfunctions $u_{n,j,l=0}(r)$ vs. \sqrt{r} choosing, for example, principal quantum numbers $n = 5, 9, 19, 29, 34, 39$, we refer to Ref. [11].
- [27] F. W. J. Olver, D. W. Lozier, R. F. Boisvert, and C. W. Clark (eds.), *NIST Handbook of Mathematical Functions* (Cambridge University Press, New York, 2010).
- [28] A. B. Migdal, *Qualitative Methods in Quantum Theory* (Addison-Wesley, Reading, MA, 1977).
- [29] E. Arimondo, M. Inguscio, and P. Violino, *Rev. Mod. Phys.* **49**, 31 (1977).
- [30] D. A. Steck, *Alkali D Line Data*, <http://steck.us/alkalidata/> (2010).
- [31] J. D. Prestage, R. L. Tjoelker, and L. Maleki, *Phys. Rev. Lett.* **74**, 3511 (1995).
- [32] B. Durand and L. Durand, *Phys. Rev. A* **33**, 2899 (1986).
- [33] A. Tauschinsky, R. Newell, H. B. van Linden van den Heuvell, and R. J. C. Spreeuw, *Phys. Rev. A* **87**, 042522 (2013).